ORIGINAL RESEARCH PAPER

IN-SITU SYNTHESIS AND CHARACTERIZATION OF CHITOSAN-Fe$_3$O$_4$ NANOPARTICLES USING TRIPOLYPHOSPHATE/CITRATE AS CROSS-LINKER

Vita T. Mardila[1], Ika O. Wulandari[1], Rizky A. Shobirin[1], Dionysius J.D.H. Santjojo[2], Akhmad Sabarudin[1*]

Brawijaya University, Faculty of Science, 65145, Malang, Indonesia
[1]*Department of Chemistry*
[2]*Department of Physics*

*Corresponding author: sabarjpn@ub.ac.id; sabarjpn@gmail.com

Abstract: One pot in-situ co-precipitation of chitosan-Fe$_3$O$_4$ nanoparticles as a candidate of drug delivery agent have been synthesized using combination of tripolyphosphate (TPP)/citrate as cross-linkers. The aim of this study was to determine the effect of preparation process towards chitosan-Fe$_3$O$_4$ nanoparticles characteristics. Chitosan-Fe$_3$O$_4$ nanoparticles were prepared on various preparation condition including Chitosan:Fe(II):Fe(III) ratio, TPP:citrate ratio, and cross-linking time. The X-ray diffraction result shows that the phase contained in nanoparticles produced is mostly Fe$_3$O$_4$ phase, since the diffraction peaks of the samples were consistent with the database in crystalline pattern of the Fe$_3$O$_4$ phase in ICSD#26410. The percentage of Fe$_3$O$_4$ was obtained from Materials Analysis Using Diffraction (MAUD) program. The presence of chitosan prevents the oxidation of Fe$_3$O$_4$, as evidenced by larger percentage of Fe$_3$O$_4$ in chitosan-Fe$_3$O$_4$ nanoparticles than bare Fe$_3$O$_4$. The combination of TPP:citrate as cross-linking agent was able to produce particles with spherical shape. Cross-linking time affect the particle size, crystallite size, and percentage of Fe$_3$O$_4$ nanoparticles. Longer duration of cross-linking process would produce the smaller particle size and crystallite size. Meanwhile, the percentage of Fe$_3$O$_4$ decreased with the increasing cross-linking time, due to the oxidation of samples in contact with the oxygen dissolved in the water.

Keywords: *chitosan-Fe$_3$O$_4$, co-precipitation, in-situ, magnetic nanoparticles*

INTRODUCTION

Magnetic nanoparticles are material consisting of magnetic elements such as iron, nickel, cobalt and its oxide with a size range of 1-100 nm which can be controlled by external magnetic field. Magnetic nanoparticles have been widely used in the biomedical field, as a drug carrier material, since it can be directed and focused on the target tissue and can be removed once therapy completed [1].

Iron oxide nanoparticles have several advantages as candidate for drug delivery system that can be visualized by magnetic resonance imaging, and also can be heated to provide hyperthermia for cancer therapy. Moreover, it can be degraded to iron ions that are not toxic in our body [2].

Preparation methods for nanoparticles were generally divided into two types: bottom-up (chemical synthesis) and top-down (mechanical attrition) processes. Among several methods of preparation iron oxide nanoparticles, co-precipitation is a bottom-up method that has a great potential due to its large-scale manufacturing, cost efficiency, and the simplicity of method. In addition, it produces hydrophilic nanoparticles that can minimize the opsonization and prolong the circulation time of the nanoparticles in the blood stream [3].

Superparamagnetic iron oxide (Fe_3O_4) is the most commonly used as drug delivery nanoparticles in biomedical applications due to its biocompatibility [4], biodegradability and simple surface modification [5]. One promising technique for nanoparticles surface modification is by coating the nanoparticles with polymers to avoid iron oxide oxidation. Some polymers used for Fe_3O_4 nanoparticles coating are polyethylene glycol (PEG), dextran, polyethyleneimine (PEI), phospholipids, and chitosan [5]. Natural polymers, such as chitosan (Ch), is highly recommended in the drug carrier systems, due to its biocompatibility and biodegradability characteristics [6].

Chitosan has the ability to interact with negatively charged (hydroxyl groups) on the surface of Fe_3O_4 nanoparticles [3]. An important aspect of chitosan as drug carrier is it can be eliminated by renal clearance, but it requires enzymatic degradation by chitinase to form smaller chain if the molecular weight is too large. The degradation rates depend on the molecular weight and the deacetylation degree of the chitosan [6]. To enhance controlled release of drug and the stability of chitosan nanoparticles drug release, chitosan can be cross-linked via both physically and chemically interaction due to the abundance of amino and hydroxyl groups of chitosan [5]. Chemical cross-linking is unfavourable for biomedical application due to the toxicity of the reagent. To overcome this adverse effect, ionic cross-linking can be employed using a negatively cross-linking agent such as tripolyphosphate and citrate [7]. The combination of TPP and citrate used in the preparation of chitosan beads obtain spherical chitosan beads [8].

In this study, chitosan-Fe_3O_4 nanoparticles were prepared *via* one pot in-situ synthesis method. The advantage of in-situ method for preparation of nanoparticle is the simplicity procedure with using mild and clean conditions to produce excellent yields [9]. Chitosan-Fe_3O_4 nanoparticles were characterized by X-Ray Diffraction (XRD), Scanning Electron Microscope (SEM), and Electron Spin Resonance Spectroscopy (ESR). The effects of preparation condition towards the characteristic of chitosan-Fe_3O_4 nanoparticles were investigated in detail. The variation of preparation parameters are Ch:Fe(II):Fe(III) ratio, TPP:citrate ratio, and cross-linking time.

MATERIALS AND METHOD

Materials

Chitosan (LMW), $FeCl_2 \cdot 4H_2O$ and tripolyphospate (TPP) were purchased from Sigma Aldrich (Singapore). $FeCl_3 \cdot 6H_2O$, CH_3COOH, $NH_3 \cdot H_2O$, and sodium citrate were obtained from Merck (Indonesia).

In-situ synthesis of chitosan-Fe₃O₄ nanoparticles

Chitosan-Fe_3O_4 nanoparticles were synthesized via in-situ co precipitation of iron salt in the presence of chitosan and cross-linker as described by Kavaz *et al.* (2010) [10] with some modification. $FeCl_2 \cdot 4H_2O$ and $FeCl_3 \cdot 6H_2O$ with ratio 1:2 (mol/mol) were dissolved in 15 mL of chitosan solution with various Ch:Fe(II):Fe(III) weight ratios (0.3:1:2.7, 0.45:1:2.7 and 0.6:1:2.7) and stirred for 30 minutes to form ferrogel. Subsequently, 5.5 mL of $NH_3 \cdot H_2O$ 3 M was added drop-wise using a syringe pump (flow rate of 10 mL·h⁻¹) to the ferrogel with constant stirring for another 30 minutes. Then, 5 mL of cross-linker was added to the mixture at a flow rate of 10 mL·h⁻¹. The mixture was then further stirred for 30 minutes. Afterwards, the colloidal chitosan-Fe_3O_4 nanoparticle produced in this stage was rinsed with distilled water until *p*H of 7 and stored at 4 °C prior to use. The obtained nanoparticles were dried using freeze dryer before characterization step.
To understand the effect of Ch:Fe(II):Fe(III) ratio, TPP:citrate ratio, and cross-linking time towards the characteristics of resulted nanoparticles, the nanoparticles were prepared according to the outlined procedures above.

Characterization of synthesized bare and chitosan-Fe₃O₄ nanoparticles

Morphological properties and particle sizes of the nanoparticles were observed through SEM images. Magnetic properties of chitosan-Fe_3O_4 nanoparticles were evaluated with ESR. Crystallite size and crystallinity of synthesized nanoparticles were analyzed by XRD (Hitachi High-Tech TM3000), and the phases of Fe_3O_4 were determined using MAUD program. The crystallite size of chitosan-Fe_3O_4 nanoparticles can be estimated by modified Scherrer's formula based on XRD data [11]:

$$\ln\beta = \ln\frac{K \cdot \lambda}{L \cdot cos\theta} = \ln\frac{K \cdot \lambda}{L} + \ln\frac{1}{cos\theta} \qquad (1)$$

where: β is the peak width of half-maximum, K is Scherrer constant, λ is the wavelength of the radiation (nm), L is the crystallite size (nm), and θ is Bragg's angle.
By plotting $\ln\beta$ against $\ln(1/cos\theta)$ (shown in Figure 1), then an intercept of $\ln K/L$ as well as the crystallite size was obtained.
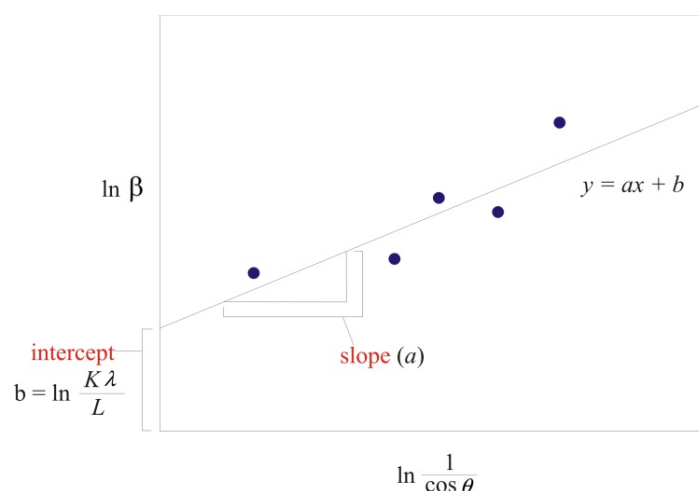
Figure 1. *Modified Scherrer equation plot*

Homogeneity of crystallite size was calculated using statistical method of Gaussian distribution shown in equation [2]:

$$(R) = \frac{1}{R} \cdot \frac{1}{2\pi \ln\left(1+\frac{\sigma_R^2}{R^2}\right)} \cdot e^{-\ln^2\left[\frac{\frac{R}{\overline{R}}\sqrt{1+\frac{\sigma_R^2}{R^2}}}{2\ln\left(1+\frac{\sigma_R^2}{R^2}\right)}\right]} \tag{2}$$

where: R is observed crystallite size, $\overline{R}$ is average crystallite size, σ is standard deviations, and π is 3.141592654.

RESULTS AND DISCUSSION

In-situ synthesis of chitosan-Fe₃O₄ nanoparticles

During the synthesis process of chitosan-Fe_3O_4 nanoparticles, Fe^{2+} and Fe^{3+} were dispersed in chitosan solution and then the ions were precipitated by the addition of $NH_3 \cdot H_2O$ (Figure 2). First, Fe^{2+} and Fe^{3+} were interacted with -OH^- from $NH_3 \cdot H_2O$ to form ferric hydroxide and ferrous hydroxide which then underwent precipitation through a very rapid reaction. Next, ferric hydroxide decomposed into FeOOH, which then reacted with $Fe(OH)_2$ and produced Fe_3O_4 (magnetite). Afterwards, amine groups in chitosan interacted with negatively charged (hydroxyl groups) on the surface of Fe_3O_4. Through this method, hydrophilic Fe_3O_4 cores formed nuclei with high surface energies, and rapidly adsorb chitosan via physical binding. The presence of chitosan around the nuclei inhibits the growth of Fe_3O_4 core, producing a smaller Fe_3O_4 core. The stoichiometric ratio of Fe^{3+}: Fe^{2+} (2:1) was applied to obtain a high purity of magnetite. The mechanism of Fe_3O_4 formation can be written in the following reactions:

$$Fe^{3+} + 3OH^- \rightarrow Fe(OH)_3 \tag{3}$$

$$Fe(OH)_3 \rightarrow FeOOH + H_2O \tag{4}$$

$$Fe^{2+} + 2OH^- \rightarrow Fe(OH)_2 \tag{5}$$

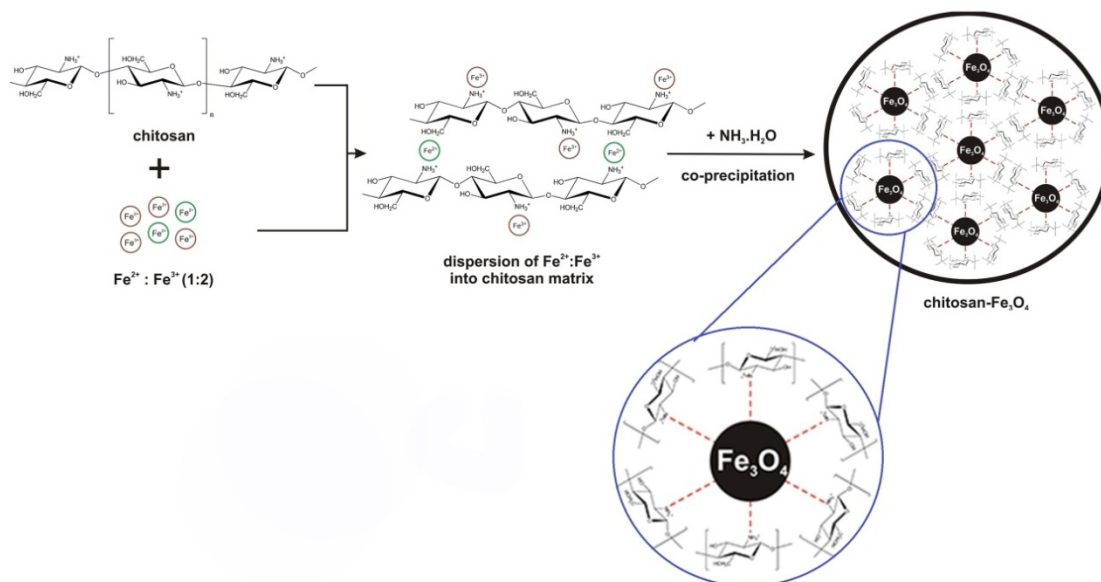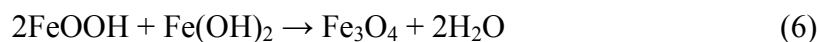$$2FeOOH + Fe(OH)_2 \rightarrow Fe_3O_4 + 2H_2O \qquad\qquad (6)$$

Figure 2. *Fe^{3+}/Fe^{2+} interaction during co-precipitation process*

The cross-linking stage begins with diffused TPP and citrate into chitosan to react with NH_3^+ group in chitosan. TPP can interact with chitosan by inter- and intramolecular ionic interaction to make chitosan structure becomes more rigid and eventually form spherical shape particles. Sodium citrate, as well as TPP, can interact with chitosan through ionic interaction as illustrated in Figure 3.
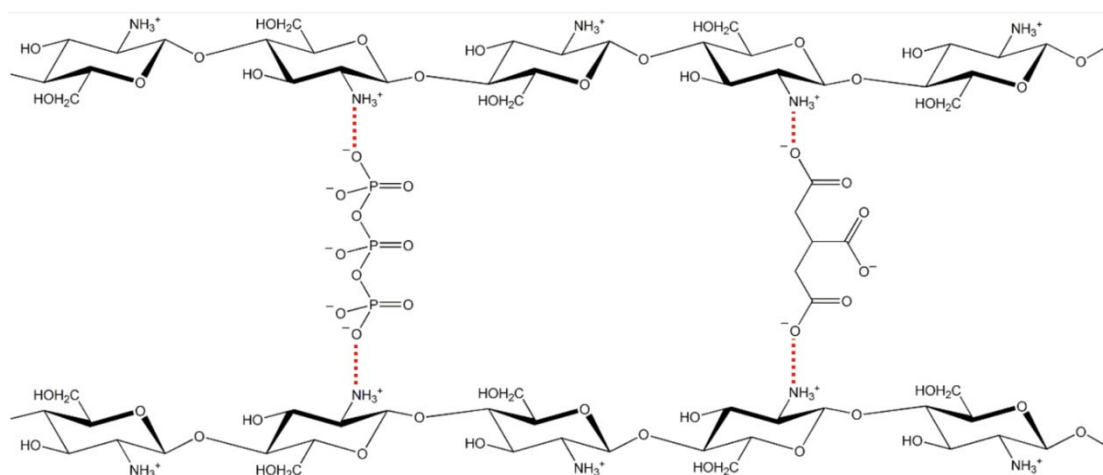

Figure 3. *TPP and citrate interaction with chitosan*

Characterization of chitosan-Fe₃O₄ nanoparticles

In the synthesis of chitosan-Fe$_3$O$_4$ nanoparticles, the effect of preparation condition such as Ch:Fe(II):Fe(III) ratio, TPP:citrate ratio, and cross-linking time was studied. The characteristics of nanoparticles were analyzed by various analytical methods.

The crystallinity of chitosan-Fe$_3$O$_4$ nanoparticles was determined by XRD. Figure 4 depicts XRD patterns of chitosan-Fe$_3$O$_4$ nanoparticles with different parameter.
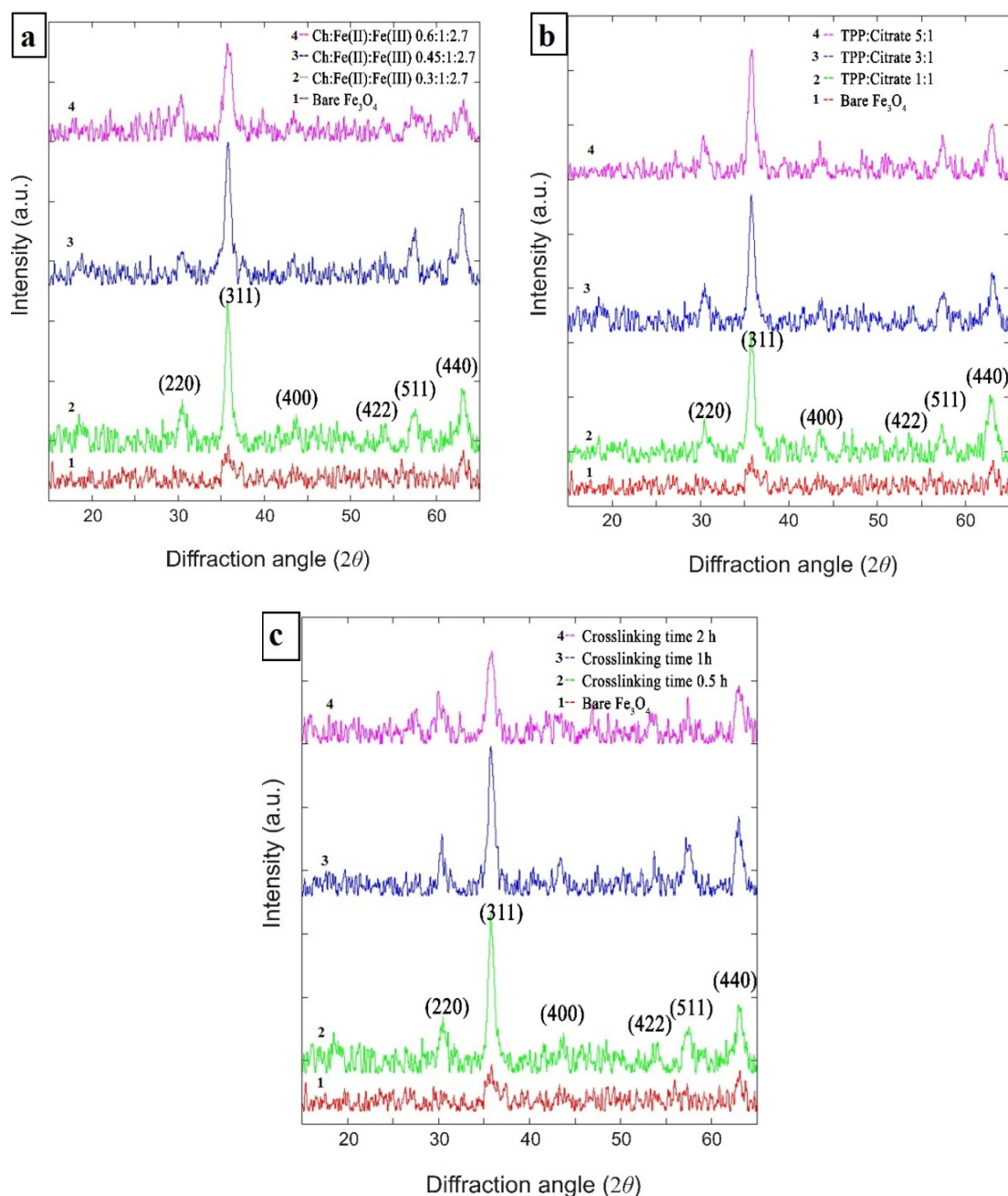

Figure 4. XRD Pattern of chitosan-Fe$_3$O$_4$ nanoparticle with variationt of:
a) ratio chitosan and iron, b) ratio cross-linker, c) cross-linking time

It is revealed that the phase in nanoparticles prepared in this study mainly consists of Fe_3O_4 phase. Diffraction peaks at (220), (311), (400), (422), (511), (440), and (533), which are the characteristic peaks of the magnetite (Fe_3O_4) were observed in samples. These peaks are consistent with the database of Fe_3O_4 properties ICSD#26410. In addition to these peaks, there are several peaks with a smaller intensity which is expected to be a maghemite (γ-Fe_2O_3) by comparison with the standard of γ-Fe_2O_3 properties ICSD#172905. This presence of maghemite can be caused by the oxidation of Fe_3O_4 by oxygen in the air or dissolved oxygen in water to form maghemite.

Figure 5 presents SEM micrographs of chitosan-Fe_3O_4 nanoparticles with different weight ratios of Ch:Fe(II):Fe(III). All of the samples have sphere structure morphology with diameter ranging from 200 to 700 nm. The particle size of chitosan-Fe_3O_4 nanoparticles is summarized in Table 1. Significant differences can be noted as size of the spheres. The diameter of chitosan-Fe_3O_4 nanoparticles is slightly bigger than bare Fe_3O_4, attributed to chitosan layer on the surface of Fe_3O_4 particles and the cluster of nanoparticles [13]. The nanoparticles tend to form clusters, which may be due to the large surface/volume ratio and intermolecular interactions, such as electrostatic, hydrophobic, and van der Waals interactions [14]. The particle size is increasing along with the increasing amount of chitosan used.
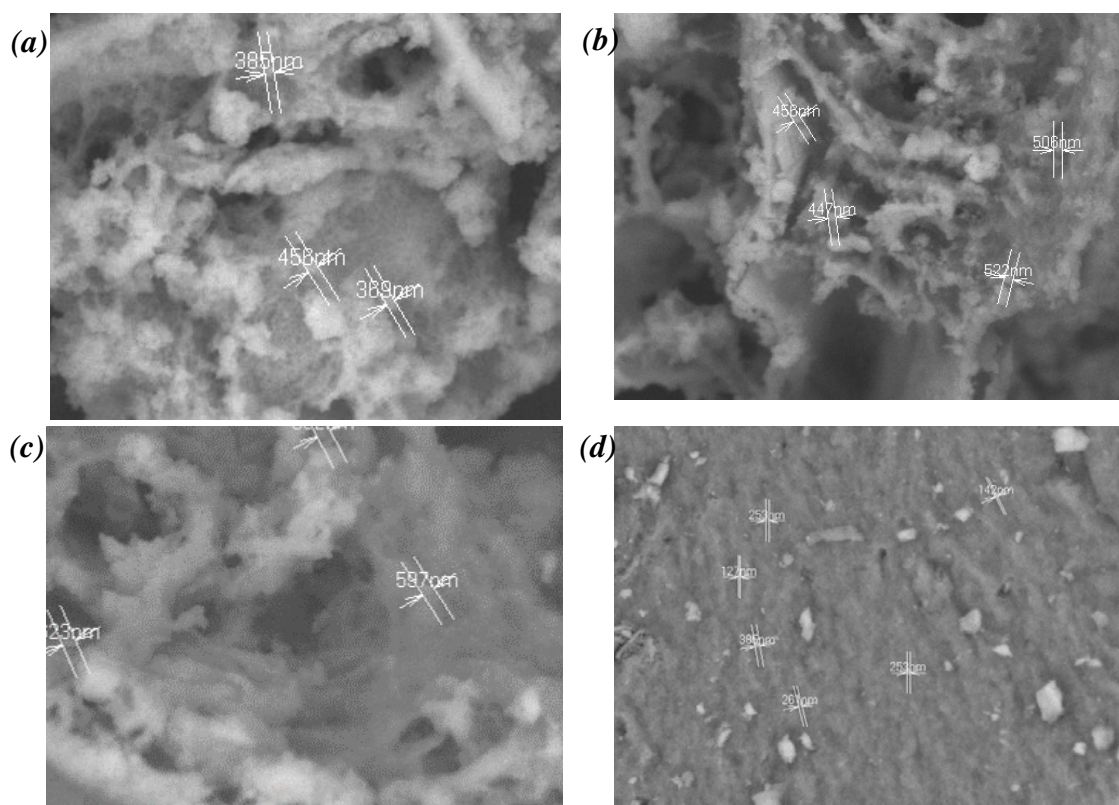

Figure 5. *SEM image of synthesized nanoparticles with different Ch:Fe(II):Fe(III) ratio*
a) 0.3:1:2.7, b) 0.45:1:2.7, c) 0.6:1:2.7, and d) bare Fe₃O₄

The amount of chitosan significantly affects the particle size, crystallite size and magnetic properties of the nanoparticles produced. The crystallite size (given in Table 1) decreased with the increasing amount of chitosan. In contrast, the particle size shows the opposite trend. This is because the chitosan inhibits the growth of Fe_3O_4 core during the synthesis process [3]. In addition, crystallite size also decreases with the increasing amount of TPP, due to the repulsion of TPP that inhibits crystal growth. According to the data listed in Table 1, cross-linking time also influences the crystallite size of nanoparticles. The longer the duration of cross-linking step, the smaller the crystallite size obtained.

Table 1. *Comparison of particle and crystallite size of chitosan-Fe_3O_4 nanoparticles*

Parameter	L^a [nm]	$(\bar{\bar{R}})^b$ [nm]	σ^c [nm]	Particle size[d] [nm]
Ch:Fe(II):Fe(III)				
0.3:1:2.7	9.49	8.4024	0.5389	229-456
0.45:1:2.7	7.5	8.5792	0.5671	456-552
0.6:1:2.7	4.94	8.9880	2.3822	679-765
TPP:citrate				
1:1	11.4	10.3633	2.1545	385-425
3:1	9.49	8.4024	0.5389	229-456
5:1	6.8	7.9433	0.6271	316-405
Cross-linking time				
0.5 h	9.49	8.4024	0.5389	226-369
1 h	7.59	7.9078	0.9443	229-456
2 h	4.41	9.8480	3.5703	152-308

[a]Unstrained crystallite size using modified Scherrer equation (Monshi *et al.*, 2012)
[b]Mean crystallite size, statistically calculated from collective data of average crystallite size using modified Scherrer equation
[c]Standard deviation
[d]measured by SEM measurement

The crystallite size distribution of nanoparticles was displayed in Figure 6. The homogeneity of crystallite size decreased with the increasing amount of chitosan used, as can be seen from Figure 6a, although crystallite size distribution between Ch:Fe(II):Fe(III) 0.3:1:2.7 and 0.45:1:2.7 did not show a significant difference. Meanwhile, it can be derived from Figure 6b that the crystallite size distribution becomes more homogeneous with the increasing ratio of TPP:citrate which indicates that the presence of TPP reinforces the degree of crystal order. The best condition was obtained in TPP:citrate ratio of 3:1. On the other hand, Figure 6c demonstrated that the longer the duration of cross-linking time, the more heterogeneous the crystallite size obtained, because there is a rearrangement among chitosans.
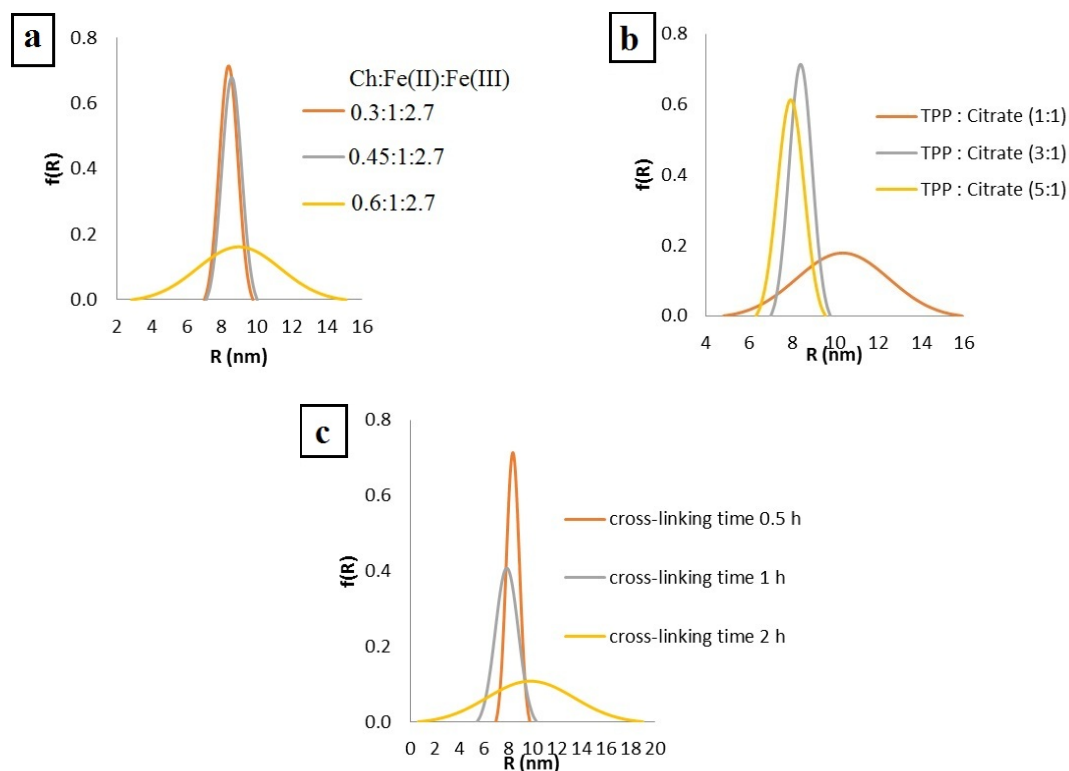
Figure 6. *Crystallite size distribution of chitosan-Fe₃O₄ nanoparticles with variation of: a) ratio chitosan and iron, b) ratio cross-linker, c) cross-linking time*

Fe_3O_4 phase in nanoparticles fabricated in this research was measured and calculated by MAUD software. The percentage of Fe_3O_4 were listed in Table 2.

Table 2. *Comparison on phase difference*

Co-precipitation method	% wt Fe_3O_4	% wt γ-Fe_2O_3
Bare Fe_3O_4	66.28	33.72
Ch:Fe(II):Fe(III)		
0.3:1:2.7	98.27	1.73
0.45:1:2.7	87.22	12.78
0.6:1:2.7	81.03	18.97
TPP:Citrate		
1:1	78.35	21.65
3:1	98.27	1.73
5:1	89.70	10.30
Cross-linking time		
0.5 h	98.27	1.73
1 h	97.62	2.38
2 h	95.42	4.68

The percentage of Fe_3O_4 decreased with the increasing amount of chitosan. However, the percentage of Fe_3O_4 in chitosan-Fe_3O_4 nanoparticles was significantly higher than bare Fe_3O_4 which indicates that chitosan can minimize oxidation of Fe_3O_4 into γ-Fe_2O_3.

From this result, it was also found that Fe_3O_4 nanoparticles contained not only Fe_3O_4 phase (magnetite) but also γ-Fe_2O_3 (maghemite), and model of its crystal structure was given in Figure 7.
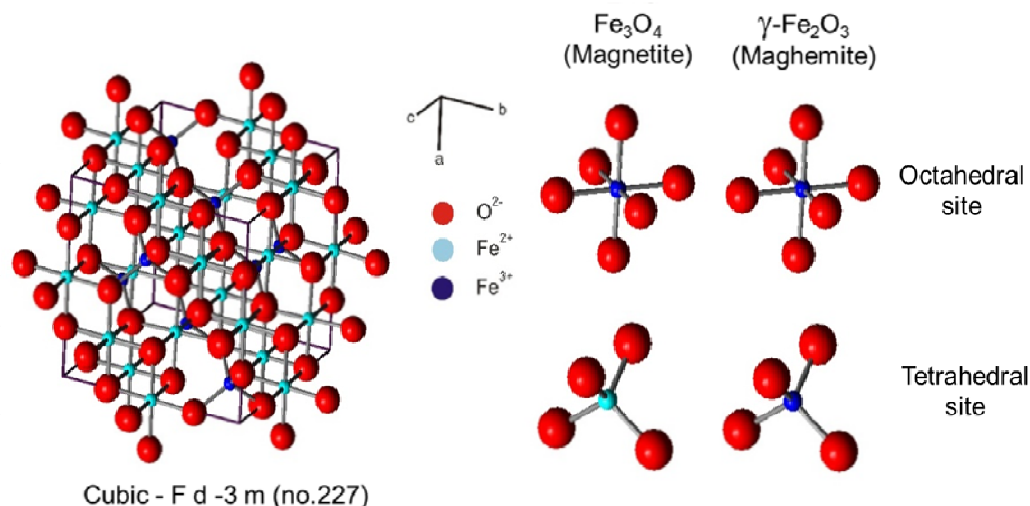

Figure 7. Crystal structure of magnetite and maghemite

Magnetic properties of chitosan-Fe_3O_4 nanoparticles were characterized using the Electron Spin Resonance (ESR) in the form of Lissajous curve. The slope of ESR curve for chitosan-Fe_3O_4 nanoparticles was given in Figure 8.
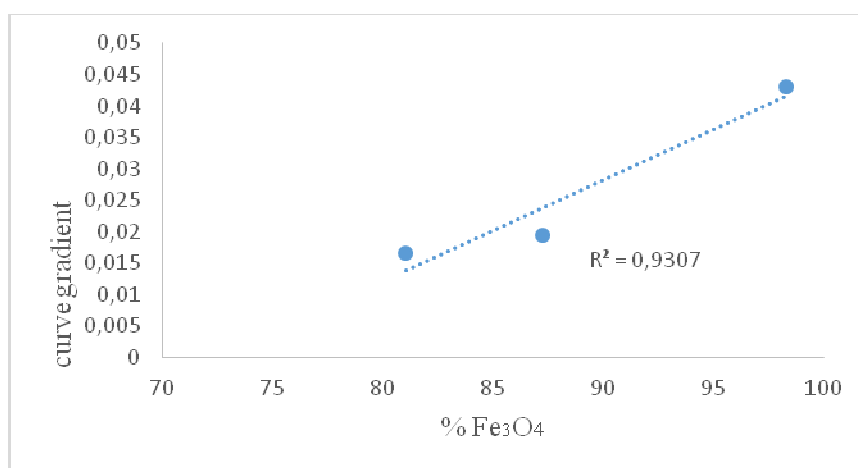

Figure 8. Correlation between % Fe_3O_4 and curve gradient ESR

The linear correlation between the slope of ESR curve and the percentage of Fe_3O_4 was observed in this research, with R^2 value of 0.93 which indicates that chitosan-Fe_3O_4 nanoparticles have significant magnetic properties that come from Fe_3O_4 particles. Chitosan-Fe_3O_4 nanoparticles have active response to the magnetic field, resulting in the higher overall system energy with the increasing of the magnetic field provided. Energy system is correspond to the amount of Fe_3O_4 phase in the sample.

CONCLUSIONS

Chitosan-Fe_3O_4 nanoparticles have been synthesized via in-situ co-precipitation. Using one-pot reaction procedure, these synthesis method have several advantages such as the simplicity and the safety of the process, because it does not use harmful organic solvents. The presence of chitosan prevent the oxidation of Fe_3O_4, in accordance with the percentage of Fe_3O_4 in chitosan-Fe_3O_4 nanoparticles which is significantly higher than those in bare Fe_3O_4. The combination of TPP:citrate as cross-linkers was able to produce particles with spherical shape. It was also revealed that the preparation process affects the characteristics of chitosan-Fe_3O_4 nanoparticles produced. The more chitosan used and the longer cross-linking time, the smaller crystallite size obtained. Magnetic property of chitosan-Fe_3O_4 nanoparticles which was measured by ESR displayed linear correlation with the percentage of Fe_3O_4.

ACKNOWLEDGMENTS

REFERENCES

1. Indira, T.K., Lakshmi P.K.: Magnetic Nanoparticles – A Review, *International Journal of Pharmaceutical Sciences and Nanotechnology*, **2010**, **3** (3), 1035-1043;
2. Hou, Y., Hao, R.: Multifunctional Nanoparticles for Multimodal Molecular Imaging (Chapter 21), in: *Nanoplatform-Based Molecular Imaging* (Editor: Chen, X), John Wiley & Sons, New Jersey, **2011**, 571-572;
3. Unsoy, G., Yalcin, S., Khodadust, R., Gunduz, F., Gunduz, U.: Synthesis Optimization and Characterization of Chitosan-Coated Iron Oxide Nanoparticles Produced for Biomedical Applications, *Journal of Nanoparticle Research*, **2012**, **14** (11), Article ID 964, 13 pages, doi:10.1007/s11051-012-0964-8;
4. Wu, W., He, Q., Jiang, C.: Magnetic Iron Oxide Nanoparticles: Synthesis and Surface Functionalization Strategies, *Nanoscale Research Letter*, **2008**, **3** (11), 397-415;
5. Arami, H., Stephen, Z., Veiseh, O., Zhang, M.: Chitosan-Coated Iron Oxide Nanoparticles for Molecular Imaging and Drug Delivery, in: *Advances in Polymer Science, Chitosan for Biomaterials I* (vol. 243), (Editors: Jayakumar, R., Prabaharan, M., Muzzarelli, R.A.A.), Springer-Verlag, Berlin, Heidelberg, **2011**, 163-184;
6. Riva, R., Ragelle, H., des Rieux, A., Duhem, N., Jérôme, C., Préat, V.: Chitosan and Chitosan Derivatives in Drug Delivery and Tissue Engineering, in: *Advances in Polymer Science, Chitosan for Biomaterials II* (vol. 244), (Editors: Jayakumar, R., Prabaharan, M., Muzzarelli, R.A.A.), Springer-Verlag, Berlin, Heidelberg, **2011**, 19-44;
7. Liu, H., Gao, C.: Preparation and Properties of Ionically Cross-Linked Chitosan Nanoparticles, *Polymer Advanced Technologies*, **2009**, **20** (7), 613-619;
8. Shu, X.Z., Zhu, K.J.: Controlled Drug Release Properties of Ionically Cross-Linked Chitosan Beads: The Influence of Anion Structure, *International Journal of Pharmaceutics*, **2002**, **233** (1-2), 217-225;
9. Zarnegar, Z., Safari, J.: Fe₃O₄@Chitosan Nanoparticles: A Valuable Heterogeneous Nanocatalyst for the Synthesis of 2,4,5-Trisubstituted Imidazoles, *RSC Advances*, **2014**, **4** (40), 20932-20939;

10. Kavaz, D., Odabaş, S., Güven, E., Demirbilek, M.., Denkbaş, E.B.: Bleomycin Loaded Magnetic Chitosan Nanoparticles as Multifunctional Nanocarriers, *Journal of Bioactive Compatible Polymers*, **2010**, <u>**25**</u> (3), 305-318;
11. Monshi, A., Foroughi, M.R., Monshi M.R.: Modified Scherrer Eqquation to Estimate More Accurately Nano-Crystallite Size Using XRD, *World Journal of Nano Science and Engineering*, **2012**, <u>**2**</u> (3), 154-160;
12. Balzar, D., Popa, N.C.: Analyzing Microstructure by Rietveld Refinement, *The Rigaku Journal*, **2005**, <u>**22**</u> (1), 16-25;
13. Ding, Y., Shen, S.Z., Sun, H., Sun, K., Liu, F., Qi, Y., Yan, J.: Design and Construction of Polymerized-Chitosan Coated Fe_3O_4 Magnetic Nanoparticles And Its Application for Hydrophobic Drug Delivery, *Materials Science and Engineering C: Materials for Biological Applications*, **2015**, <u>**48**</u>, 487-498;
14. Asmatulu, R., Fakhari,A., Wamocha, H.L., Chu, H.Y., Chen, Y.Y., Eltabey, M.M., Hamdeh, H.H., Ho, J.C.: Drug-Carrying Magnetic Nanocomposite Particles for Potential Drug Delivery Systems, *Journal of Nanotechnology*, **2009**, <u>**2009**</u>, Article ID 238536, 6 pages, http://dx.doi.org/10.1155/2009/238536.